Exhaust Manifold Design with Tapered Pipes Using Divided Range MOGA[1]

Masahiro Kanazaki[2] , Shigeru Obayashi[3] and Kazuhiro Nakahashi[4]

Summary

Multiobjective design optimization system of exhaust manifold shapes with tapered pipes for a car engine has been developed by using Divided Range Multiobjective Genetic Algorithm (DRMOGA) to obtain more engine power as well as to produce less pollutant. Although the present design problem is known highly nonlinear, the exhaust manifold has been successfully designed to improve both objectives. The comparison of the results obtained by DRMOGA and MOGA was performed and DRMOGA was demonstrated to find better solutions than MOGA.

1. Introduction

To improve intake/exhaust system performance of a car engine, many design specifications are required. In addition, car engines today are required not only to have more engine power, but also to be more environmentally friendly. Exhaust gas should be kept in high temperature in the exhaust pipe especially at low rpm conditions when engine starts because the catalyst located at the end of the exhaust pipe will absorb more pollutant in high temperature conditions. Exhaust gas should also be led from the piston chambers to the exhaust manifold smoothly to maximize the engine power especially at high rpm conditions. Such design is used to be performed by trial and error through many experiments and analyses by engineers. Therefore, an automated design optimization is desired to reduce technical, schedule, and cost risks for new engine developments.

In the previous study, the exhaust manifold for the high power engine shown in Fig. 1 was considered and the merging configurations of the exhaust manifold and its pipe radius (a single parameter for the entire manifold) were designed to optimize the interaction of the exhaust gas around junctions of the manifold [1]. The objective functions were to maximize the gas temperature at the end of the exhaust pipe at 1,500 rpm and to maximize the charging efficiency that indicates the engine power at 6,000 rpm. Many solutions achieved higher engine power as well as less environmental impact compared to the initial geometry.

According to the previous study, a larger radius of the manifold was effective to keep the gas temperature higher, while such design candidates have less engine power. To compromise both effects, this study will make the pipes' radii increase gradually as they merge together. Such design is more realistic and known to perform well by experiences at industry. Objective functions considered here are the same as the previous study.

In this study, the automated design optimization system is developed by using DRMOGA [2]. DRMOGA is characterized by the parallelization model where the individuals are divided into subpopulations. DRMOGA is known to enhance the population diversity and to produce better nondominated solutions. The subdivision of the population based on alternative objective functions prevents the premature convergence to a nondominated solution segment and introduces migration of individuals to neighboring nondominated solution segments. A comparison of results produced by DRMOGA and previous MOGA was also performed to verify the performance of the optimization of DRMOGA for the

1. Manuscript received on

2. Graduate Student, Tohoku University.

3. Professor, Institute of Fluid Science, Tohoku University.

4. Professor, Dept. of Aeronautics and Space Engineering, Tohoku University.

practical application.

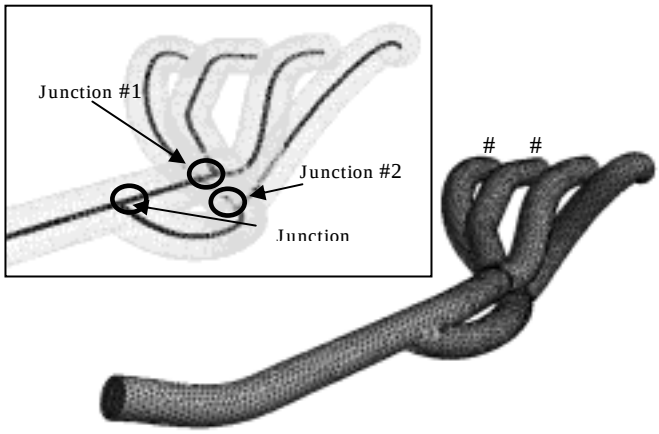

Fig.1: The initial manifold shape and design variables as junction positions on pipe centerlines.

2. Formulation of the optimization problem

2.1 Objective functions The objective functions considered here are to maximize the gas temperature at the end of the exhaust pipe at 1,500 rpm and to maximize the charging efficiency at 6,000 rpm, where the charging efficiency indicates the engine power. These two objectives are function of a flow past the exhaust pipe over an engine cycle.

2.2 Divided Range Multiobjective Genetic Algorithm DRMOGA procedure shown in Fig. 2 can be explained as follows. First, initial individuals are produced randomly and evaluated. Second, the division of individuals is performed by using the rank of individuals based on values of a certain objective function *fi*. Assuming m subpopulations for *N* individuals, N/m individuals will be allocated to each subpopulation. Then in each subpopulation, the existing MOGA is performed. In this study, MOGA utilized real-number cording [3], the Pareto ranking method [4], BLX-0.5 [3] and Best-N selection [5] and mutation rate was set to 0.1. After MOGA is performed for k generations, all of the individuals are gathered and they are divided into subpopulations again according to the ranking based on another objective function *fj*. This ranking function will be chosen in turn. For present DRMOGA, *k* was set to 4 and number of subpopulation m was set to 4.

2.3 Evaluation A flowfield in a manifold is computed by solving an unsteady three-dimensional inviscid flow code [6]. Unsteady boundary conditions for a flow to and from a manifold are simultaneously computed by using the one-dimensional, empirical engine cycle simulation code [1, 7]. Function evaluations in MOGA were parallelized on SGI ORIGIN2000 supercomputer system at the Institute of Fluid Science, Tohoku University. Evaluation time of a single manifold design was about 20 hours by using a single CPU of ORIGIN2000.

2.4 Geometry definition To define manifold geometry automatically, merging points and pipe radius should be determined first. Figure 3 illustrates how to define a merging point and pipe radius by using BLX-0.5.

The pipe centerline is labeled by points when points $p1$ and $p2$ were selected as parents, children $c1$ and $c2$ are to be determined as,

$$c1=\gamma\times p1+(1-\gamma)\times p2$$
$$c2=(1--\gamma)\times p1+\gamma\times p2 \quad (1)$$
$$\gamma=(1+2\alpha)ran-\alpha$$

where α is the indicator of BLX-α and set to 0.5 in this study and *ran* is a random number.

Pipes radii of children are also defined from parents' radii by using BLX-0.5. Figure 3(b) illustrates the definition of pipe radius of a child.

To generate a computational grid according to given design variables, an automated procedure to find a pipe junction from pipe centerlines was developed in the previous study [1] as shown in Fig. 4. The pipe centerlines are reconstructed from the merging points and temporary background grids are generated for each pipe segment from the given centerlines and pipe radius. Then the overlap region of the pipes is calculated and removed. The advancing-front method [8] is applied to generate the computational surface grid by specifying the junction as a front. With this method, various merging configurations can be generated only by specifying the merging points on the pipe centerlines.

In this study, the initial manifold shape is taken from an existing engine with four pistons as shown in Fig. 1.

Topology of the merging configuration is kept unchanged. The pipe shape traveling from the port #2 to the outlet is also fixed. Three merging points on the pipe centerlines, junctions #1-3, are considered as design variables. Pipe centerlines of #1, 3 and 4 are then deformed similarly from the initial shapes to meet the designed merging points. The pipe shapes are finally reconstructed from the given pipe radius. This method allows the automated grid generation for arbitrary merging configuration defined by the pipe centerlines.

This study considered three design cases. The first case assumes a constant pipe radius 17.5 cm for all pipes, therefore only three merging points are to be designed. This is referred as Case 1.

In the second case, three merging points and the pipe radius of the entire exhaust manifold are to be designed, and thus the number of design variable is four. The pipe radius will vary from 83% to 122% of the original radius. This is referred as Case 2. These two cases are computed for comparison purposes.

In the last case, the pipe radii are increased when pipes merge at junctions. Because pipe radii are defined at three regions as shown in Fig. 5, the number of design variables is six: three merging points, radius r_0 defined at the region 1 and the increments of radius a and b defined at regions 2 and 3, respectively. Manifold's geometry has a taper with increasing the pipe radius linearly at a junction. Figure 6 illustrates how to define the taper geometry of a pipe at the junction. In this study, the pipe radius r_0 will vary from 90% to 120% of the original radius, the increment a will vary from 0.9 to 1.18 and the second increment b will vary from 0.9 to 1.23. These values were determined based on the industrial experience. This is referred as Case 3.

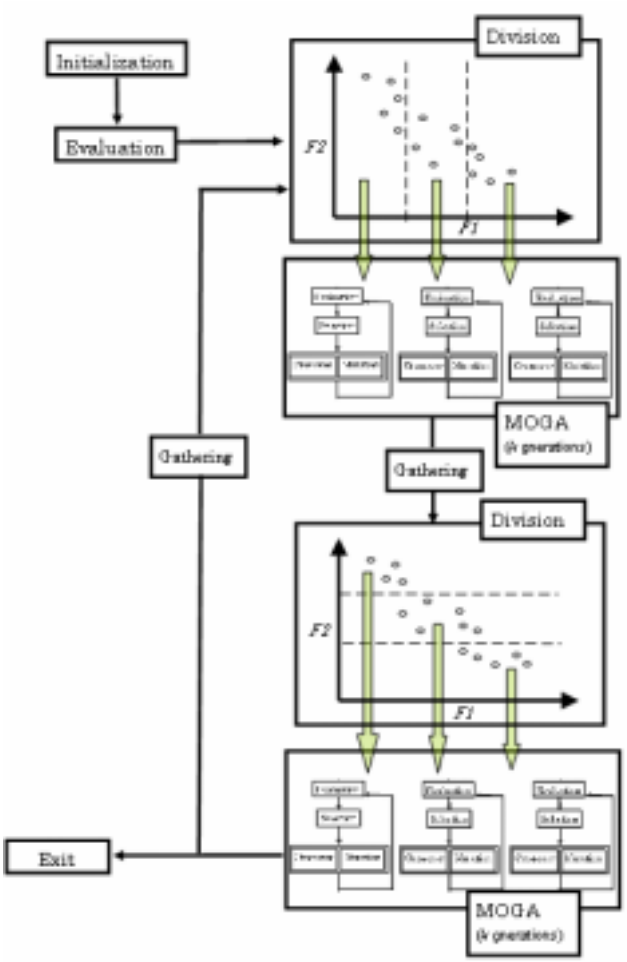

Fig. 2: Procedure of DRMOGA.

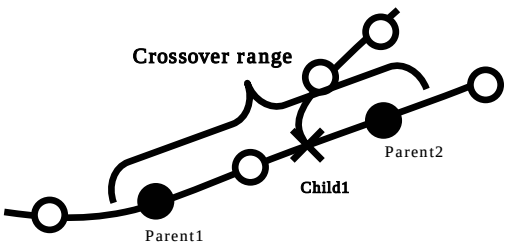

(a)

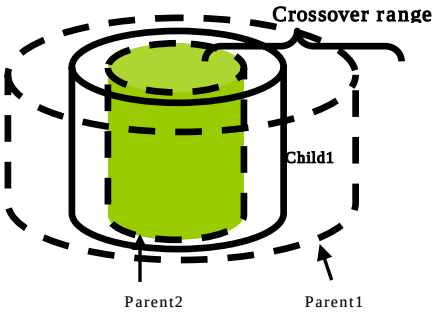

(b)

Fig.3: Illustration of parameter crossover by using BLX-0.5; (a) merging point and (b) pipe radius.

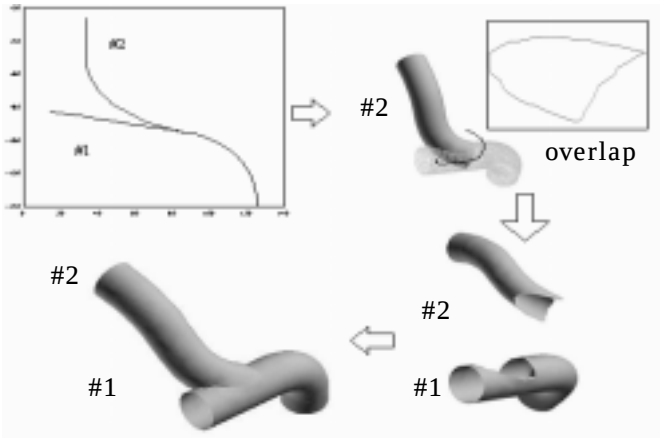

Fig.4: Surface definition with arbitrary pipe junction.

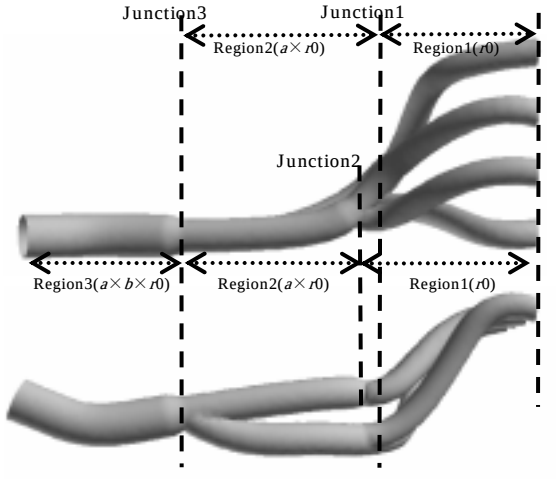

Fig.5: Radius definitions for a manifold with tapered pipes.

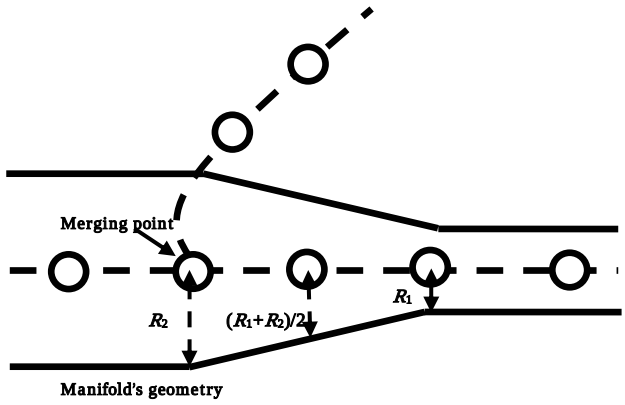

Fig. 6: Tapered geometry definition at a merging point.

3. DESIGN OPTIMIZATION OF AN EXHAUST MANIFOLD

3.1 Design problems In this study, three design problems were considered. First, the design optimizations of merging points were performed (Case 1). Second, merging points and pipe radius were designed (Case 2). Finally, the merging points and pipe radii were optimized with changing pipe radii as pipes merge (Case 3).

Population sizes were 32 for Case 1 and 64 for Cases 2 and 3. For all cases, the evolution was advanced for 36 generations and subpopulations were reconstructed every 4 generations.

3.2 Optimization results of merging configuration design (Case 1) In Case 1, nondominated solutions were found as shown in Fig. 7. Many manifold shapes achieve much higher charging efficiency than the initial geometry. These results suggest that the design of merging points is effective to improve in the charging efficiency that indicates the engine power. However, the improvement in the temperature remained marginal.

Manifold geometries taken from two nondominated solutions are shown in Fig. 8. It was difficult to find simple correlations between design variables and the charging efficiency. It suggests that the design variables have strong interactions and that the resulting charging efficiency is highly nonlinear.

3.3 Optimization results of merging configuration and constant pipe radius design (Case 2) In Case 2, nondominated solutions were found as shown in Fig. 9. Good improvement in the gas temperature was achieved and the improvement in charging efficiency was almost the same as Case 1. This result suggests that the design of pipe radius can produce manifold shapes achieving higher gas temperature without reducing the charging efficiency.

Trends of top 100 individuals sorted by Pareto ranking are shown in Fig. 10, where the gas temperature and the charging efficiency are plotted as a function of the pipe radius, respectively. Solid lines are regression lines. As the pipe radius increases, the gas temperature is fond to increase in general, while the charging efficiency decreases.

Manifold geometries taken from two nondominated solutions are shown in Fig. 11. The solution C achieved very high charging efficiency and the solution D achieved the highest temperature. The radius of the solution D became larger, and thus it achieved higher temperature. On the other hand, its charging efficiency was not improved very much. Although the solution C achieved much higher charging efficiency, its radius was almost identical with the initial shape. These results suggest that the large radius through the manifold is effective to maximize the gas temperature but it has a tradeoff in the charging efficiency.

3.4 Optimization results of merging configuration and variable pipe radius design with tapered pipes (Case 3) In Case 3, from the observation about the influence of the constant radius design presented in section 3.3, the design of the variable pipe radii at pipe junctions was performed to maximize the charging efficiency furthermore.

In Case 3, nondominated solutions were found as shown in Fig. 12. Almost all manifold shapes achieve higher charging efficiency and temperature than the initial geometry. Nondominated solutions are found to achieve higher charging efficiency than those in Case 2. This result shows that the variable pipe's radii at junctions are very effective to increase the charging efficiency furthermore.

Trends of top 100 individuals sorted by Pareto ranking are shown in Figs. 13-15. Influences of the radius determined in region 1 in gas temperature and charging efficiency are shown in Fig. 13, respectively. These figures showed same trends presented in section 3.3. However more individuals achieved higher charging efficiency than those in Fig. 10. This result suggests the advantage of the tapered pipe. Figure 14 shows influences of the first increment a and Fig. 15 shows influences of the second increment b. According to these figures, as the increments a and b increase, the charging efficiency became higher and the gas temperature became lower. These result suggest that the tapered pipe introduced by the increments a and b is effective to maximize the charging efficiency but is not good for the gas temperature.

To summarize, the gas temperature can be maximized with the large radius. But the charging efficiency will be penalized when the pipe radius increases constantly. Thus, the tapered pipe with the increments a and b at junctions is necessary to maximize the charging efficiency. Both objective functions can be maximized successfully by using the tapered pipe.

Manifold geometries taken from two nondominated solutions are shown in Fig. 16. The solution E achieved the highest charging efficiency and the solution F achieved the highest temperature. The solution E also achieved much higher temperature than the initial shape. Radii of solution E and F became larger, and thus it

achieved high temperature. On the other hand, only the solution E was improved in the charging efficiency. The difference between the solutions E and F is the radius variation. The radius of solution E was increased at each junction resulting in the tapered pipe. On the other hand, the radius of solution F was almost constant similar to Case 2. These results agree with the observation in Fig. 13.

3.5 Comparison of nondominated solutions in three cases Figure 17 shows that the comparison of nondominated solutions in three cases. From this figure, the results in Cases 1, 2 and 3 can be summarized as follows. The design of merging configuration performed in Case 1 is effective to maximize the charging efficiency. The merging configuration and pipes radii performed in Case 2 can maximize not only the charging efficiency but also the exhaust gas temperature. However the constant large radius pipe penalizes the charging efficiency. The design of the variable pipe radii performed in Case 3 can produce much higher charging efficiency than any other cases while keeping the gas temperature high.

3.6 Comparison of solutions obtained by DRMOGA and MOGA In this study, the manifold design was also performed by using the previous MOGA without subpopulations [9] for Case 3. The comparison of solutions obtained by DRMOGA and MOGA is shown in Fig. 18. Both cases were evaluated for 36 generations starting from the same initial population.

According to these solutions, the solutions obtained by DRMOGA showed more diversity than the solutions by MOGA. The nondominated solutions found by DRMOGA also outperformed those obtained from MOGA. These results suggest that DRMOGA can maintain more diversity in the population and produce better nondominated solutions.

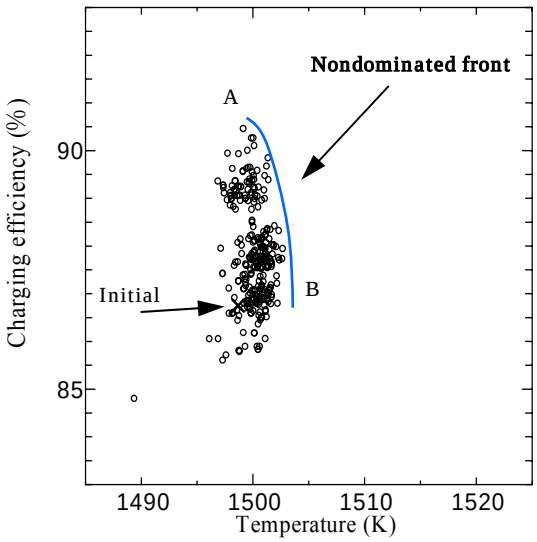

Fig. 7: All manifold solutions produced by DRMOGA in Case 1.

A Maximum charging efficiency

B Maximum temperature

Fig. 8: Manifold shapes of selected nondominate solutions in Case 1; merging points' optimization.

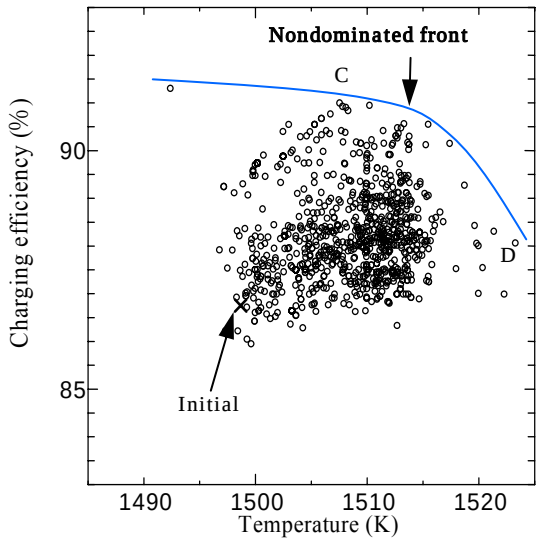

Fig. 9: All manifold solutions produced by DRMOGA in Case 2.

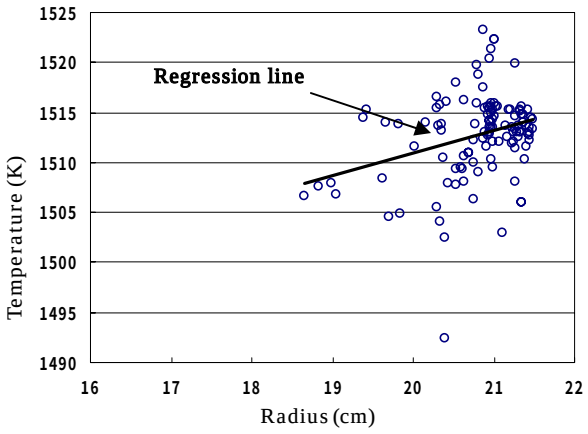

(a)

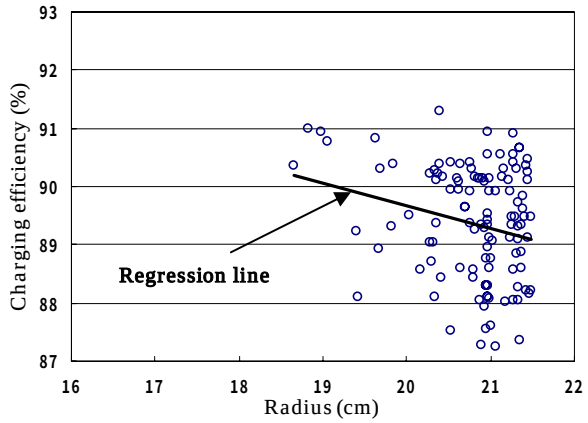

(b)

Fig. 10: Performance of top 100 individuals as a function of the pipe radius; (a) Gas temperature, (b) Charging efficiency.

C. Selected solution from nondominate front

D. Maximum temperature

Fig. 11: Manifold shapes of selected from nondominate solutions in Case 2; merging points and constant radius optimization.

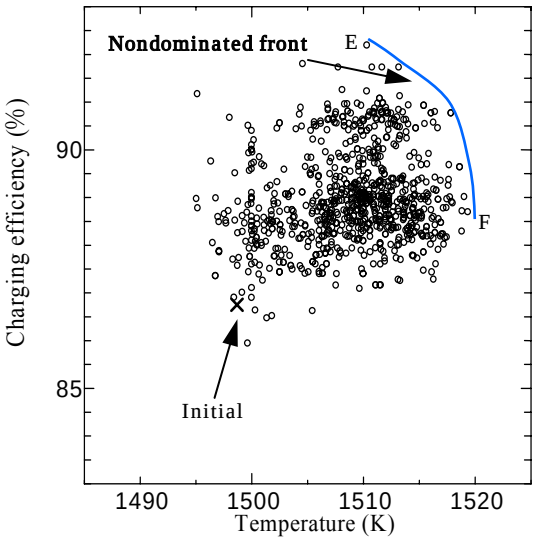

Fig. 12: All manifold solutions produced by DRMOGA in Case 3.

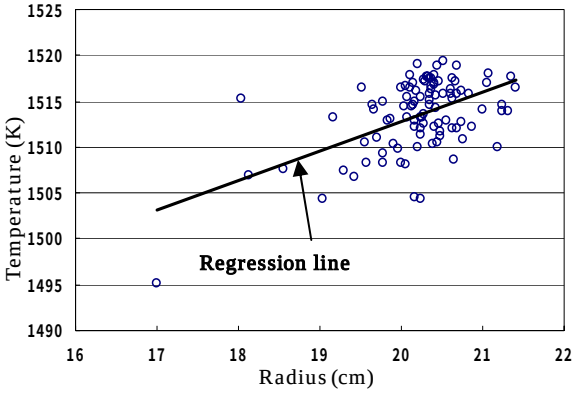

(a)

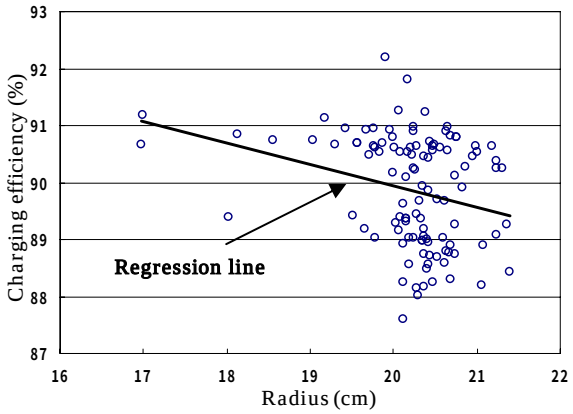

(b)

Fig. 13: Performance of top 100 individuals as a function of the pipe radius; (a) Gas temperature, (b) Charging efficiency.

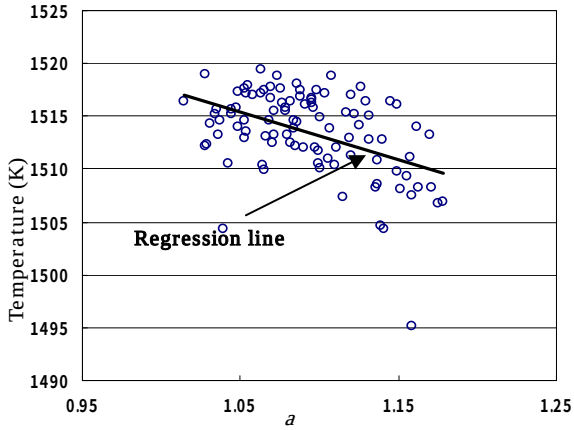

(a)

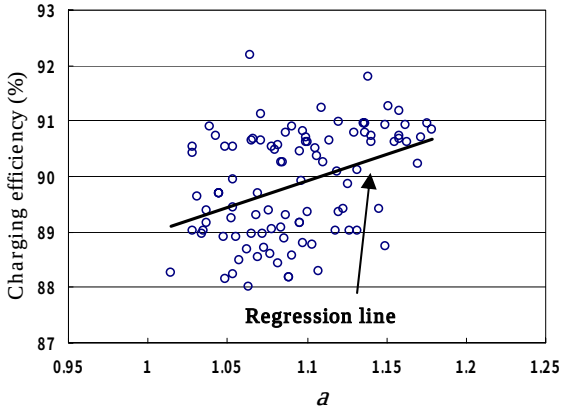

(b)

Fig. 14: Performance of top 100 individuals as a function of the first radius increment *a*; (a) Gas temperature, (b) Charging efficiency.

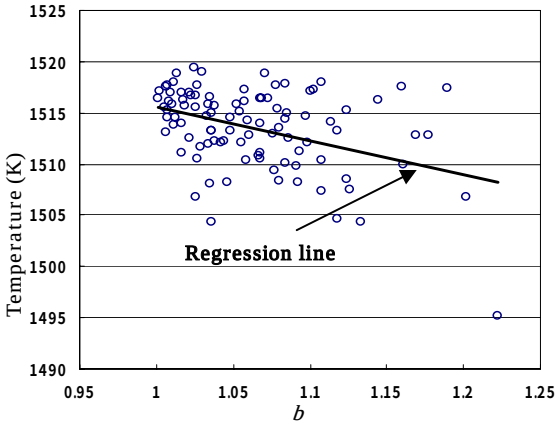

(a)

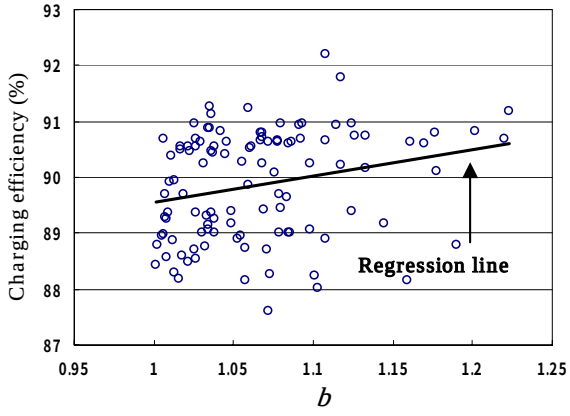

(b)

Fig. 15: Performance of top 100 individuals Performance of top 100 individuals as a function of the second radius increment *b*; (a) Gas temperature, (b) Charging efficiency.

E Maximum charging efficiency

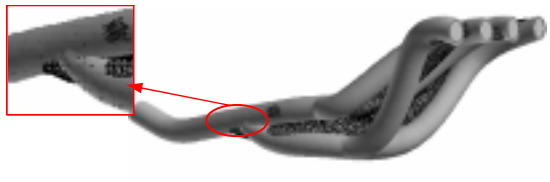

F Maximum temperature

Fig.16: Manifold shapes of selected nondominate solutions in Case 3; merging points and variable radius optimization.

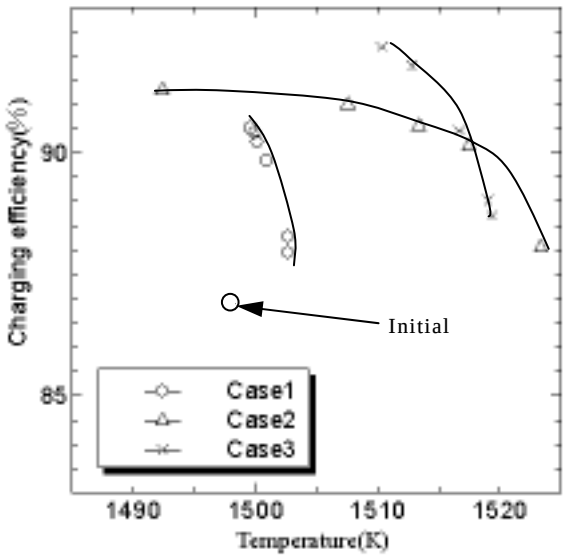

Fig.17: Comparison of nondominated solutions in three cases.

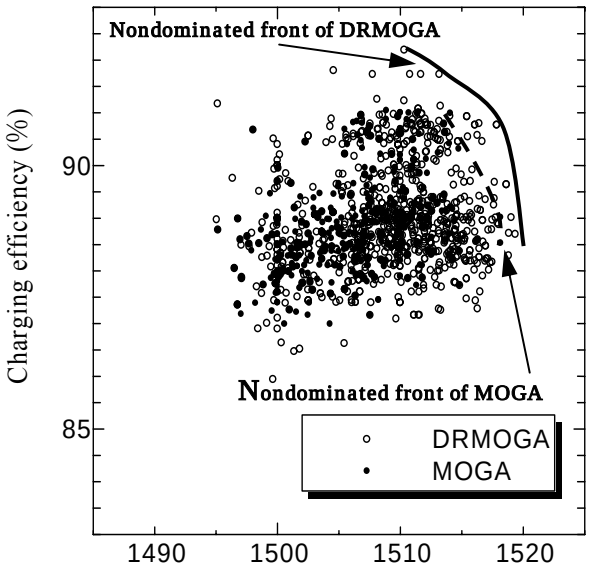

Fig. 18: Comparison of all manifold shapes obtained by DRMOGA and MOGA.

4. Concluding remarks

An improved design optimization system of an exhaust manifold of a car engine has been developed by using DRMOGA. In this automated design system, the empirical car engine cycle simulation code was coupled with the unstructured, unsteady Euler code for evaluation of a flow through the three-dimensional manifold shapes. Computational grids were automatically generated from the designed merging points on pipe centerlines. The initial configuration of the manifold was taken from an existing high power engine with four cylinders.

At first, the manifold shape was optimized by three merging points on the pipe centerlines, assuming the pipe radius constant. The present system found nondominated solutions mainly improved in the charging efficiency. This result suggests that the merging configuration is effective to improve the charging efficiency.

The second case optimized both the pipe radius and merging points. The present system successfully found nondominated solutions improved in the both objective functions considered in this study. Although larger pipe radius gives higher temperature, it is also found to have a tradeoff in the charging efficiency.

In the last optimization problem, the manifold is divided into three regions based on merging points and

pipe radii are given separately. In this case, almost all nondominated solutions appear better than the initial design and most of them achieve higher charging efficiency than the nondominated solutions in former cases. This result suggests that the variable pipe radius definition is an important design specification to achieve further improvements in the charging efficiency. The present system has successfully found solutions that have less environmental impact and more engine power simultaneously than the initial design.

This paper also presented the comparison the solutions obtained from DRMOGA and MOGA. DRMOGA is demonstrated to perform better than MOGA in the practical application.

5. Acknowledgements

We would like to thank Powertrain Research Laboratory in Mazda Motor Corporation for providing the one-dimensional empirical engine cycle simulation code and the engine data. The calculations were performed by using the supercomputer, ORIGIN 2000 in the Institute of Fluid Science, Tohoku University.

References

[1] M. Kanazaki, S. Obayashi and K. Nakahashi: Multiobjective Design Optimization of Merging Configuration for an Exhaust Manifold of a Car Engine, *Proc. PPSN, the 7th international conference on parallel problem solving from nature*, (2002), p.p.281-287.

[2] T. Hiroyasu, M. Miki and S. Watanabe: The New Model of Parallel Genetic Algorithm in Multi-Objective Optimization Problems (Divided Range Multi-Objective Genetic Algorithm), *IEEE Proc. the Congress on Evolutionary Computation 2000,* Vol.1 (2000), p.p.333-340.

[3] L. J. Eshelman and J. D. Schaffer: Real-coded genetic algorithms and interval schemata, *Foundations of Genetic Algorithms2,* Morgan Kaufmann Publishers, Inc. (1993), p.p. 187-202.

[4] C. M. Fonseca and P. J.Y. Fleming: Genetic algorithms for multiobjective optimization, *Proc. 5th International Conference on Genetic Algorithms*, (1993), p.p. 416-423.

[5] K. A. De Jong: An Analysis of the Behavior of a Class of Genetic Adaptive System, Doctoral Dissertation, (1975), University of Michigan, Ann Arbor.

[6] D. Sharov and K. Nakahashi: Reordering of 3-D Hybrid Unstructured Grids for Lower-Upper Symmetric Gauss-Seidel Computations, *AIAA J.*, Vol.36(1998), No.3, p.p.484-486.

[7] K. Ohnishi, H. Nobumoto, T. Ohsumi, and M. Hitomi: Development of Prediction Technology of Intake and Exhaust System Performance Using Computer Simulation, *MAZDA Technical Paper* (*in Japanese*), Vol.6 (1998), p.p.84-93.

[8] Y. Ito and K. Nakahashi: Direct Surface Triangulation Using Stereolithography (STL) Data , *AIAA Paper*, (2000)No. 2000-0924.

[9] M. Kanazaki, S. Obayashi and K. Nakahashi: The Design Optimization of Intake/Exhaust Performance of a Car Engine Using MOGA, *Evolutionary Methods for Design, Optimization and Control, Proc. EUROGEN2001*, (2001), p.p.423-428.